International Journal of Biology and Life Sciences
ISSN: 2957-9511 | Vol. 2, No. 1, 2023

Immunogenic cell death-related classification to predict prognosis and immunotherapeutic response in hepatocellular carcinoma

Xinyang Cao*, Zhang Yu

School of Chemical Engineering and Pharmacy, Jingchu Institute of Technology, Jingmen, Hubei, China 44800

* **Corresponding author**: Xinyang Cao (Email: 2044703802@qq.com)

Abstract: Immunogenic cell death (ICD) has been classified as a form of regulated cell death (RCD) sufficient to activate adaptive immune responses. There is growing evidence that ICD is capable of reshaping the tumor immune microenvironment through the release of danger signals or DAMPs, which may contribute to immunotherapy. Currently, identification of ICD-related biomarkers that allow patients to benefit from ICD immunotherapy would be of great help to classify patients. Here, we identified two subtypes associated with ICD by consensus clustering. high ICD subtypes were associated with good clinical outcome, immune cell infiltration and immune response signaling activity. In addition, we developed and validated an ICD-related prognostic model that predicted survival in HCC and correlated with the tumor immune microenvironment. In conclusion, we developed a new ICD subtype-based classification system for HCC. This classification has significant clinical outcomes for assessing prognosis and of immunotherapy of HCC patients.

Keywords: Immunogenic cell death; HCC; Tumor microenvironment; Liver cancer prognosis; Immune cell infiltration.

1. Introduction

The low immunogenicity and immune escape of tumors make it difficult for the body to generate a sustained immune response, which is the main cause of tumor recurrence and metastasis. It has been found that in addition to direct cytotoxicity, some chemotherapeutic drugs induce immunogenic cell death (ICD) through various mechanisms, releasing damage-associated molecular patterns (DAMPs) and enhancing anti-tumor immune effects. Enhancement of antitumor immune effects. Early exposure to endoplasmic reticulum calreticulin (CRT) on the cytosolic surface, extracellular secretion of adenosine triphosphate (ATP), heat shock protein (HSP)-antigenic peptide complexes and late release of high mobility group protein B1 (HMGB1) in DAMPs are the main causes of immunogenicity in ICDs. Tumor immunotherapy is a therapeutic approach to control and clear tumors by restarting and maintaining the tumor-immune cycle and restoring the body's normal anti-tumor immune response. The activation of ICD's to clear tumors is receiving more and more attention to scientists. Existing ICD models are not sufficient to support their application of the clinic, and therefore patients need to be evaluated before having a clinical background for the possibility of ICD. The discovery of specific biomarkers is of great importance for the application of ICD immunotherapy.

Hepatocellular carcinoma (HCC) is one of the leading causes of cancer death worldwide, often with low survival rates and poor quality of life at advanced stages. The current treatment strategies to deal with hepatocellular carcinoma include hepatectomy, liver transplantation, translator arterial chemo embolization (TACE), ablation therapy, radiation therapy, systemic therapy, and combination therapy, which can prolong the survival time of hepatocellular carcinoma. Among the immunotherapies for hepatocellular carcinoma, atelelizumab + bevacizumab, pablizumab, carrilizumab and nabritumomab + epilimumab are the most representative. The continued development of cancer immunotherapy and greater understanding of the response to T cell-targeted immune checkpoint therapy, as well as the development of drugs to block these immune checkpoint agents, will allow for vigorous development of immunotherapy and biomarker discovery for HCC.

In the current study, we aim to identify ICD-related biomarkers and develop an ICD risk model to predict the immune microenvironment, prognosis and response to immunotherapy in HCC. In the future, this technology could help physicians make important judgments on treatment.

2. Materials and Methods

Data set: RNA-seq transcriptome information and matched clinicopathological data onto 110 HCC patients were obtained by downloading from TCGA (https://portal. Gdc Cancer Gov/) , sett numbers <10 as cancer group and >10 as normal group , yielding a total of 109 cancers samples and 1 normal sample .

Consensus clustering: Consensus clustering was performed using the ConsusclusterPlus tool of R to identify molecular subtypes associated with ICDs. Subsequently, we evaluated the ideal number of clusters of k=2-10 and repeated the process 1000 times to ensure stable results. pheatmap tool of R was used to create cluster maps.

Identification of differentially expressed genes (DEGs): differential mRNA expression was assessed using the Limma package of R software (version: 3.40.2). To correct for false-positive TCGA data, adjusted P values were examined. screening criteria for differential expression of mRNAs was determined as adjusted $P<0.05$ and $|\log2 FC|>2$.

Functional enrichment analysis: For gene set functional enrichment analysis we used the GO annotation of genes from the R package org. Hs Eg Db (version 3.1.0), the KEGG rests API (https://www.kegg.Jp/kegg/rest/keggapi Html) to obtain the latest KEGG Pathway's gene annotation was used as the background to map the genes into the background set and

enrichment analysis was performed using the R package cluster Profiler (version 3.14.3) to obtain the results of gene set enrichment. A minimum gene set of 5 and a maximum gene set of 5000 were set, and a P value of < 0.05 and an FDR of < 0.25were considered statistically significant.

Gene pooling enrichment analysis (GSEA): GSEA software (version 3.0) was obtained from the GSEA (DOI: 10.1073/pnas.0506580102, http ://software. Broadinstitute.org/gsea/index Jsp) website , and the samples were divided into two groups according to high and low ICD subtypes , divided the samples of two groups , and downloaded c2 . Cp from Molecular Signatures Database (DOI: 10.1093/bioinformatics/btr260, http://www.gsea-msigdb#org/gsea/downloads.Jsp). The kegg. V7.4 Symbols Gmt subset was downloaded from the Molecular Signatures Database (DOI: 10.1093/bioinformatics/btr260, COPY) to assess relevant pathways and molecular mechanisms based on gene expression profiles and phenotypic groupings, sett a minimum gene set of 5 and a maximum gene set of 5000, with one thousand resamplings , and a P value of < 0.05 and an FDR of < 0.25 was considered statistically significant .

Immune landscape characterization between the two ICD subgroups: To determine the immune characteristics of 110 HNSCC samples, their expression data were loaded into CIBERSORT (HTTPS://CIBERSORT.stanford.edu/) and repeated 1000 times to determine the relative percentages of 22 immune cell types. We then compared the relative percentages of the 22 immune cell types between the two ICD subgroups and the results are shown in the landscape plots.

Prediction of immunotherapy response: Tumor Immune Dysfunction and Exclusion (TIDE) analysis has been used to determine immunotherapy response.TIDE (http://tide.dfci.harvard.edu/) is an analytical technique that allows the prediction of immunotherapy response using two major mechanisms of tumor immune evasion: suppression of T cells in tumors with low CTL levels dysfunction and T-cell infiltration.

Somatic mutation analysis: Somatic mutation data for HCC samples were obtained in "maf" format from the TCGA GDC data portal. Waterfall plots were then performed using the "Maftools" package in R software, which facilitates the visualization and summarization of mutated genes.

Survival analysis: Kaplan-Meier (KM) analysis was performed to compare overall survival (OS) between the low-ICD risk cohort and the high-ICD risk cohort, using survminer and maxstat in R (maximally selected rank statistics with several p-value approximations version: 0.7-25) Prognostic prognostic indicators were determined using univariate Cox analysis, whereas whether risk scores was an independent risk factor of HCC OS was determined using multivariate Cox analysis.

Construction of risk characteristics associated with ICD: Immune-related genes found to be statistically significant in univariate Cox regression analysis were subsequently exposed to LASSO-Cox regression analysis to calculate the exact coefficient values for each identified association. LASSO is a commonly used regression analysis method that combines variable selection and regularization to improve the predictive performance and interpretability of the resulting statistical model. LASSO is a common regression analysis method that combines variable selection and regularization to improve the predictive performance and interpretability of the resulting statistical models.

3. Results

3.1. Consensus clustering identified two subtypes associated with ICD

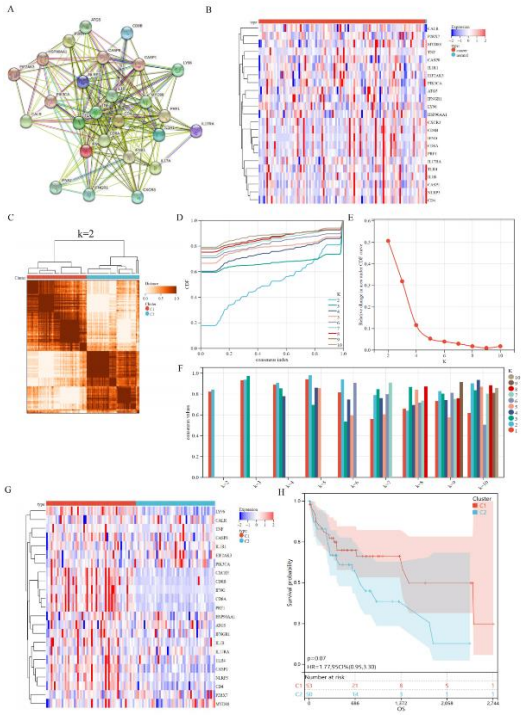

Figure 1 Identification of ICD-associated subtypes by consensus clustering. (A) Protein-protein interactions between ICD-associated genes; (B). Heat map showing ICD gene expression profiles in normal and HCC samples from the TCGA database; (C). Heat map depicting the consensus clustering solution (k=2) of genes in HCC samples, the matrix contains a total of 109 samples of 23 genes; (D-F) clustering analysis: D cumulative distribution curve, E: area under the distribution curve, F: sample clustering consistency analysis; (G). Heat map of ICD-related gene expression of different subtypes. Red indicates high expression, blue indicates low expression; (H). Survival curves. Red indicates high expression, blue indicates low expression.

You may insert up into 5 heading levels into your manuscript as can be seen in " Styles " tab of this template. These formatting styles are meant as a guide, as long as the heading levels are clear, Frontiers style will be applied during typesette. ICD-related genes have been reported on / to a large literature and summarized by Abhishek et al. Protein-protein interaction (PPI) networks / networked analysis was performed using the STRING database to further to reveal the network of relationships of / to / between these ICD-related genes, with CASP8, HSP90AA1 and CD8A interactions being the most closely related in the reciprocal network, with scores of 0.965, 0.900 and 0.884, respectively (Figure 1A). We also analyzed the expression patterns of ICD genes in normal and HCC samples. Some ICD genes were overexpressed in HCC, including CALR, CASP8, EIF2AK3, PIK3CA, CD8A, ATG5, and HSP90AA1 (Figure 1B). Next, HCC clusters associated with ICD were identified using consensus clustering analysis. The area under the CDF curve was evaluated based on the area under the CDF curve, which gradually increased with increasing k. The area under the curve was evaluated based on the decreasing trend of CDF Delta, which kept the slowest decreasing Delta, while keeping the area under the curve as large as possible. Overall, C1 showed high expression of ICD-related genes, indicating a

high ICD subtype. In contrast, C2 showed low expression levels, indicating low ICD subtypes (Figure 1G). Therefore, we defined C1 as the high ICD subtype and C2 as the low ICD subtype. Furthermore, survival analysis showed that these ICD-based subtypes exhibited different clinical outcomes. Overall, the low-ICD subtype had a poor prognosis and the high-ICD subtype was associated with a better clinical prognosis (Figure 1H).

3.2. Identification of differentially expressed genes (DEGs) and signaling pathways to different ICD subtypes

Because of the good clinical prognosis of the high ICD subtype and the poor prognosis of the low ICD subtype, we need to understand the key DEGs and signaling pathways to each subtype to understand the molecular mechanisms regulating their prognosis. The differential analysis yielded a collection of 2143 deregulated genes (Figure 2A , B) , and the unregulated genes in the high ICD subtype were enriched with genes that can regulate immune activity , including mediating immune regulation , cytokine and cytokine receptor regulation , chemo kine regulation , natural killer cell-mediated , T cell receptor regulation , and differentiation regulation of Th1 and Th2 cells (Figure 2C , D) . These results suggest that high subtypes of ICD are associated with an immune active microenvironment.

To further to identify the relevant signaling pathways activated in the high ICD subgroup, we performed a GSEA comparison between the high and low ICD subgroups. differential enrichment analysis of the gene set in the ICD group yielded a total of 186 cellular pathways, and the three highest scoring pathways was Natural killer cell mediated cytotoxicity, Cell adhesion molecule and Cheekiness signaling pathway, all associated with immune regulation (Figure 2E).

3.3. Somatic mutations and tumor microenvironment landscape in ICD high and ICD low subtypes

There were obvious somatic mutations between the high ICD subtype and low ICD subtype (Figure 3A, B). Although TP53, TTN, CTNNB1, MUC16 and ALB were obvious mutations and AXIN1, ARID1A, HMCN1, CACNA1E and RYR1 mutations were not obvious, the mutation frequencies differed from / with subtypes. the expression of regulatory genes such as tumor suppressor proteins, cell growth and intercellular adhesion in ICD high subtype, such as TP53 and CTNNB1, etc . be significantly more frequently mutated than into the low ICD subtype, while the mutation frequency of genes encoding actin was significantly higher in the low ICD subtype than in the high ICD subtype, eg., TTN.

High ICD expression has a significant impact on the activation of certain anti-tumor immune responses. In analyzing the results of the tumor microenvironment of both subtypes, it was shown that the stromal score, immune score and tumor purity were higher in the ICD high subtype compared to the ICD low subtype (Figure 4A). Next, we assessed the differences in immune infiltration of 22 immune cells between the two subtypes using the CIBERSORT method and the LM22 feature matrix. Figure 4B summarizes the results of 110 HCC patients in TCGA. Specifically, patients with high ICD subtypes had B cells naive, T cells CD8 , T cells CD4 memory resting , T cells follicular helper , NK cells resting , Macrophages M1 , Dendritic cells resting and Mast cells activated percentages were significantly higher , while T cells CD4 naive among them had no effect (Figure 4C) . In addition, both leukocyte antigen (HLA) genes and immune checkpoints were unregulated in the high ICD subtype defining this as an immune hot phenotype, while both were down regulated in the low ICD subtype defining it as an immune cold phenotype (Figure 4D, E).

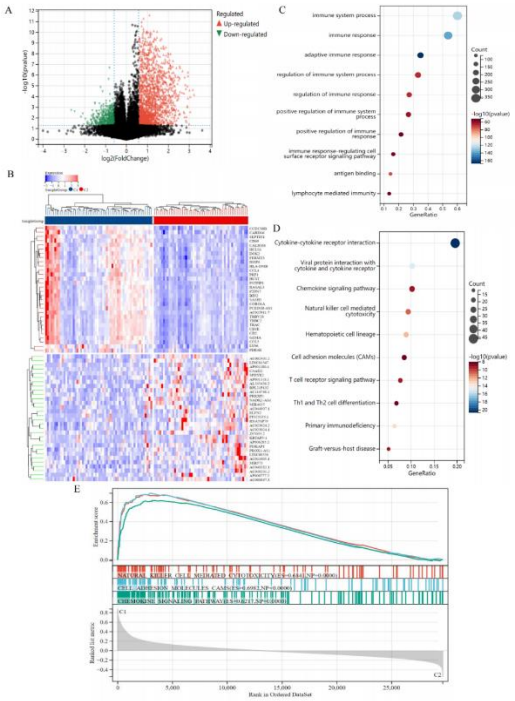

Figure 2 Identification of differentially expressed genes (DEGs) and potential signalling pathways in different subtypes. (A) Volcano plots showing the distribution of DEGs quantified between ICD high and ICD low subtypes in the TCGA cohort with a threshold of $|\log^2|>1$, $p<0.05$; (B) Heat map showing the expression of DEGs in different subtypes; (C) Dots plot showing the enrichment analysis of GO signalling pathways. The size of the dots indicates gene counts and the colour of the dots indicates -$\log_{10}$; (D) Dots plot showing enrichment analysis of the KEGG signaling pathway. The size of the dots indicates gene counts, and the colour of the dots indicates -$\log_{10}$ (p. adjust-value); (E) GSEA analysis to identify potential signaling pathways to ICD high and ICD low subtypes.

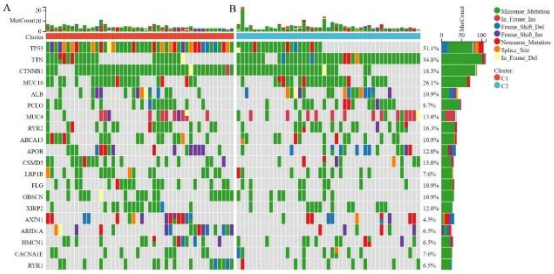

Figure 3 Comparison of somatic mutations between different ICD subtypes. (A, B) ICD high subtype (A) and ICD low subtype (B).

3.4. Construction and validation of ICD risk characteristics

A prognostic model predicated on ICD-related genes was developed. The prognostic significance in the characterized samples was assessed using the Cox method, and the overall prognostic difference significance was as follows: logtest=1.401e-14, sctest=3.887e-14 and waldtest=1.094e-06 with a C-index of: 0.897. A total of 18 ICD-related sequences

were identified (AC245100.3, PHBP3, AL512652.2, LINC02256, GAD1, PREB, AL132780.4, LDAH, AL513548.1, PSMD1, PSD4, RTN3, PHKA2, SYBU, ABCD1, PTMAP4, DTYMK, PPIAP30) were significantly associated with OS of patients (Figure 5A). Integrating survival time, survival status and gene expression data, regression analysis was performed using the lasso-cox method. In addition, we set a 5-fold cross-validation to obtain the optimal model. We set the Lambda value to 0.169 and finally obtained 18 sequences (Figure 5B, C). The risk scoring model was developed based on the following algorithm.

RiskScore=0.034*ABCD1+0.090*AC245100.3+0.124*AL132780.4+0.491*AL512652.2-0.241*AL513548.1+0.205*DTYMK+0.046*GAD1+0.003*LDAH-0.392*LINC02256+2.624*PHBP3+0.045*PHKA2+0.305*PPIAP30+0.104*PREB-0.025*PSD4+0.098*PSMD1+0.075*PTMAP4+0.030*RTN3-0.028*SYBU.

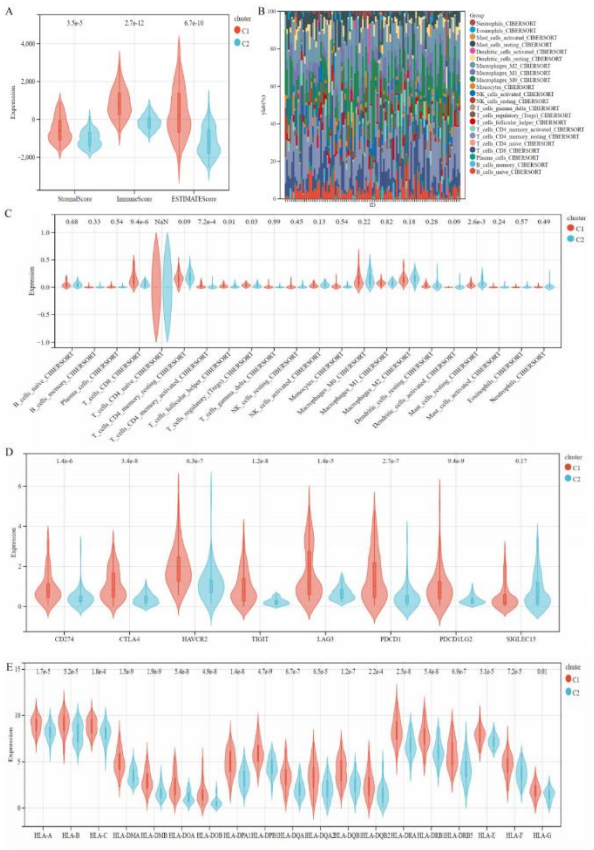

Figure 4 Immune landscape of ICD high and ICD low subtypes. (A) Violin plots showing stromal fraction, immune fraction and tumour expression fraction; (B) relative proportion of immune infiltration in ICD high and ICD low subtypes (C) Violin plots showing the level of immune cell epigenesis between different subtypes (D, E) Violin plots showing differential expression of multiple immune checkpoints (D) and HLA genes (E) in ICD high and ICD low subtypes.

To further investigate the relationship between survival status and risk scores. The relationship between different risk scores and patients' follow-up time, events and changes in the expression of each gene was analyzed, and it was observed that the survival rate of patients decreased significantly with increasing risk scores, as expected LINC02256, AL513548.1, PSD4 and SYBU were protective factors, with a down-regulation trend in expression with increasing risk scores, PHBP3, AL512652.2, GAD1, PREB, AL132780.4, LDAH, PSMD1, RTN3, PHKA2, ABCD1, PTMAP4, and DTYMK were risk factors and showed an up-regulation trend in expression with increasing risk score. (Figure 5D). The optimal cut-off value of RiskScore was calculated using the R package maxstat, setting the minimum grouping sample size greater than 25% and the maximum sample size grouping less than 75%, and the final optimal cut-off value was obtained as: 9.828, based on which the patients were divided into high and low groups, and the prognostic differences between the two groups were further analyzed using the survfit function of the R package survival, using the The logrank test method was used to assess the significance of the prognostic difference between the two sample groups, which finally

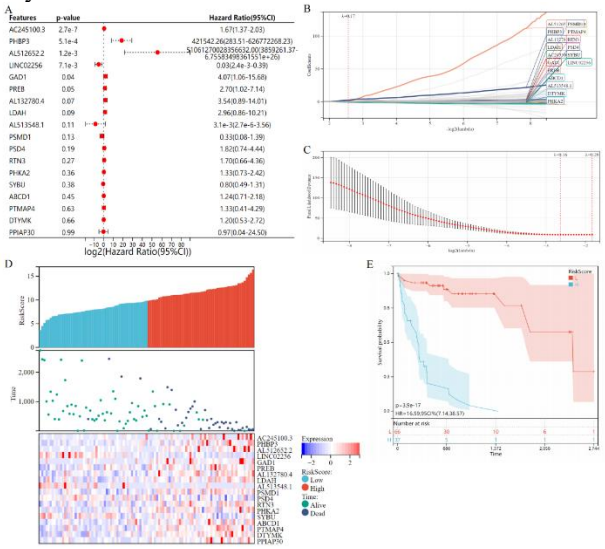

Figure 5 Construction and validation of the ICD risk profile. (A) Univariate Cox analysis to assess the prognostic value of ICD genes in terms of OS; (B, C) Lasso-Cox analysis to identify the 18 genes most associated with OS in the TCGA dataset; (D) Heat map of the distribution of risk scores, survival status and prognosis of each patient in the TCGA database for 12 genetic features; (E) Kaplan-Meier analysis to demonstrate the prognostic significance of the risk model in the TCGA cohort.

yielded a significant prognostic difference between the high and ground expression groups (p=1.4e-18) (Figure 5E), with high risk scores corresponding to poorer OS in the TCGA cohort.

3.5. Correlation between ICD risks characteristics with tumor microenvironment.

In view of the important biological role of ICD in the antitumor immune response, the relationship between ICD risk scores and the tumor microenvironment was investigated in depth. The results showed that patients with elevated risk scores were negatively correlated with B cells naive, T cells CD4 memory resting and Macrophages M1, and positively correlated with Macrophages M0, T cells gamma delta and T cells CD4 memory activated (Figure 6A). Univariate Cox assessed prognostic significance in a sample of 103, and overall prognostic differences were significant as log test=6.079e-16, sc test=1.800e-15 and wald test=1.902e-11 with a C-index of: 0.842, indicating that high ICD risk scores were significantly associated with poor OS (Figure 6B).

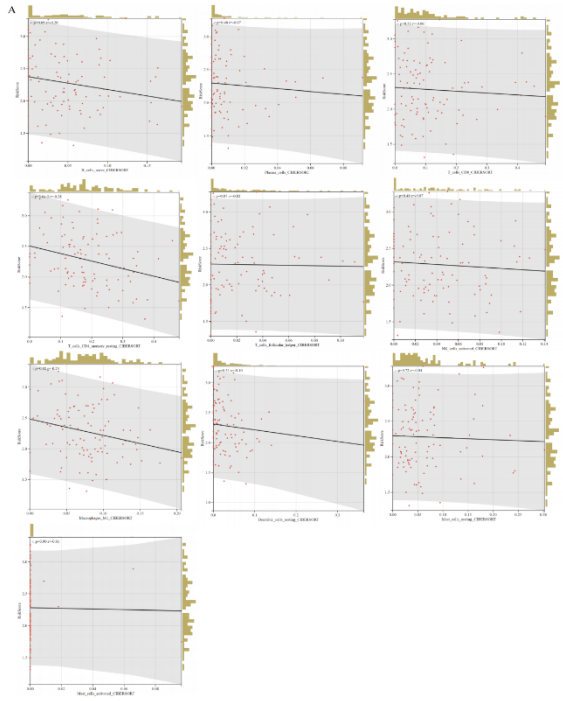

(A)

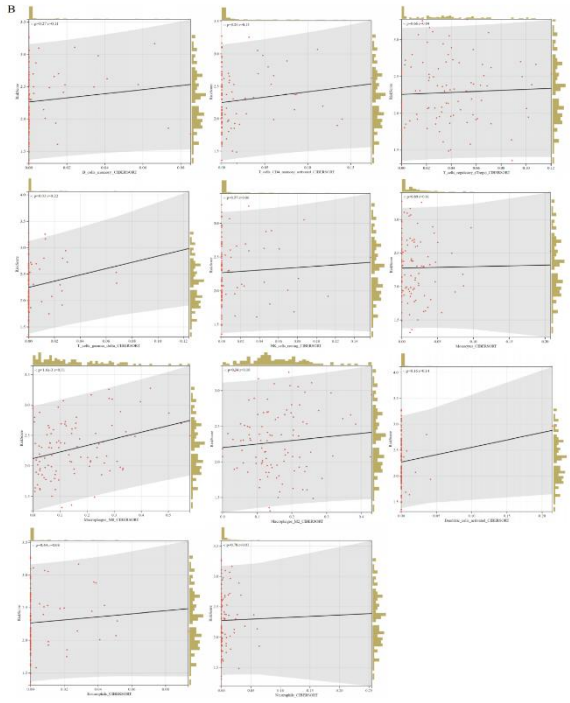

(B)

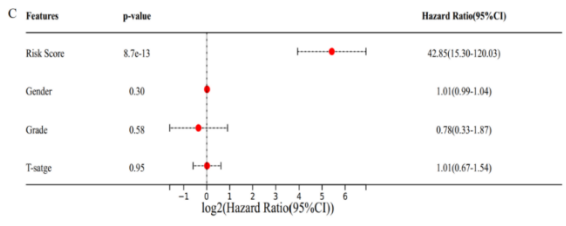

(C)

Figure 6 Correlation of ICD risk characteristics with the tumour microenvironment. (A) Scatterplot showing negative correlation between risk score and immune cell infiltration. (B) Scatter plot showing positive correlation between risk score and immune cell infiltration. (C) Univariate Cox

4. Discussion

ICD is a specific variant of Regulated cell death (RCD), driven by stressful stress, that induces adaptive immunity against dead cell antigens. The combination of immunogenic therapy and immunotherapy with each other has brought new directions in the treatment of malignancies. Thus, with the benefit of immunotherapy in mind, the identification of ICD-associated biomarkers can help differentiate HCC patients and play a crucial role in precision medicine. Here, we demonstrate that the expression of ICD-related genes is closely associated with the prognosis and tumor microenvironment of HCC. We identified two ICD subgroups by consistent clustering based on ICD-related gene expression. high ICD subtypes were associated with good clinical outcome and high levels of immune cell infiltration.

Seven of the 23 ICD-related genes showed upregulation trends in HCC patient samples, including CALR, CASP8, EIF2AK3, PIK3CA, CD8A, ATG5, and HSP90AA1, with CASP8, HSP90AA1, and CD8A being the most strongly associated in ICD gene interactions. The expression of ICD in the samples was divided into ICD high expression group and ICD low expression group based on consensus clustering analysis and CDF curves below. low ICD subtypes had poor prognosis and high ICD subtypes were associated with better clinical prognosis. In the analysis of ICD-regulated cellular pathways, it was found that the ICD-based effects of HCC were all in immune aspects, and the major somatic significant mutation sites in the high ICD subtype were tumor suppressor protein, cell growth and intercellular adhesion regulatory genes, while the effects on tumor microenvironment were that ICD mediated immune regulation, cytokine and cytokine receptor regulation, chemokine regulation, natural killer cell-mediated, T cell receptor regulation, and differentiation of Th1 and Th2 cells, stromal score, immune score, and tumor purity were higher in ICD high subtypes compared to ICD low subtypes, and immune infiltration of 22 immune cells in patients with ICD high subtypes had B cells naive, T cells CD8, T cells CD4 memory resting, T cells follicular helper, NK cells resting, Macrophages M1, Dendritic cells resting and Mast cells activated percentages were significantly higher in patients with high ICD subtypes, and both leukocyte antigen (HLA) genes and immune checkpoints were upregulated in high ICD subtypes thus ICD high subtype is an immune fever phenotype.

Significant prognostic differences existed on the ICD characteristic samples, and overall significant prognostic differences were obtained for 18 ICD-related sequences: AC245100.3, PHBP3, AL512652.2, LINC02256, GAD1, PREB, AL132780.4, LDAH, AL513548.1, PSMD1, PSD4 RTN3, PHKA2, SYBU, ABCD1, PTMAP4, DTYMK, PPIAP30 .5A). After integrating survival time, survival status and gene expression data, regression analysis was performed using the lasso-cox method, which also yielded 18 correlation sequences in agreement with the above. Combining the relationship between different risk scores and the follow-up time , events and changes in expression of individual genes of patients , it was concluded that the survival rate of patients decreased significantly from / to increasing risk scores , LINC02256 , AL513548.1 , PSD4 and SYBU were protective factors and showed a down-regulation trend in expression with increasing risk scores , PHBP3 , AL512652.2 GAD1 , PREB , AL132780.4 , LDAH , PSMD1 , RTN3 , PHKA2 , ABCD1 , PTMAP4 , and DTYMK were risk factors , and the

expression showed an up-regulation trend with increasing risk scores . An in-depth study between ICD risks score and tumor microenvironment concluded that patients with elevated risk score were associated with B cells naive, T cells CD4 memory resting and Macrophages M1 were negatively correlated and positively correlated with Macrophages M0, T cells gamma delta and T cells CD4 memory activated. Univariate Cox analysis yielded that high ICD risk scores were significantly associated with poor OS.

Immunogenic cell death (ICD) triggered by cancer therapy reshapes the tumor immune microenvironment. Mechanistically, ICD coincides with the exposure and release of many DAMPs, which facilitates their interaction with the cognate PRR displayed by the intrinsic immune cells. This leads to the activation and maturation of these cells, which metastasize into lymph nodes filled with a specific payload of cancer-derived antigens. The subsequent exposure to tumor antigens to T cells leads to enhanced infiltration of immune cells into the tumor microenvironment. Based on this evidence, our study identified two ICD subgroups by consistent clustering, with the high ICD subgroup associated with an immune hot phenotype and the low ICD subgroup referred to as the immune cold phenotype.

In conclusion, our study highlights the relevance to ICD subtypes to changes in the immune tumor microenvironment of HCC. These observations may be useful for immunotherapeutic interventions in HCC patients. We also constructed and validated ICD-related prognostic features, which are of great value of predicting the OS time in HCC patients. In conclusion, our study highlights the relevance to ICD subtypes to changes in the immune tumor microenvironment of HCC. These observations may be useful for immunotherapeutic interventions in HCC patients. We also constructed and validated ICD-related prognostic features, which are of great value of predicting the time of OS in HCC patients.

Data Availability Statement

In this study, publicly available datasets were analyzed. These data can be found here: https://portal.gdc.cancer.gov/ (TCGA-HCC)

Authors' contributions

The study involving human participants was reviewed and approved by the Ethics Review Committee of Harbin Medical University. Written informed consent is not required for this study in accordance with national laws and institutional requirements. In accordance with national laws and institutional requirements, written informed consent is not required for this study.

References

[1] Abdul Wahab SM, Jantan I, Haque MA,et al. Exploring the Leaves of Annona muricata L. as a Source of Potential Anti-inflammatory and Anticancer Agents. Front Pharmacol. 2018 Jun 20;9:661.

[2] Yang PM, Hsieh YY, Du JL, Yen SC, Hung CF. Sequential Interferon β-Cisplatin Treatment Enhances the Surface Exposure of Calreticulin in Cancer Cells via an Interferon Regulatory Factor 1-Dependent Manner. Biomolecules. 2020 Apr 21;10(4):643.

[3] Yeung HY, Lo PC, Ng DK,et al.. Anti-tumor immunity of BAM-SiPc-mediated vascular photodynamic therapy in a BALB/c mouse model. Cell Mol Immunol. 2017 Feb;14(2):223-234.

[4] Cui G, Wu J, Lin J, Liu W,et al.. Graphene-based nanomaterials for breast cancer treatment: promising therapeutic strategies. J Nanobiotechnology. 2021 Jul 15;19(1):211.

[5] Wang Y, Sun H, Xiao Z, et al.. XWL-1-48 exerts antitumor activity via targeting topoisomerase II and enhancing degradation of Mdm2 in human hepatocellular carcinoma. Sci Rep. 2017 Aug 30;7(1):9989.

[6] Tsuchiya K, Kurosaki M, Sakamoto A, et al., On Behalf Of Japanese Red Cross Liver Study Group. The Real-World Data in Japanese Patients with Unresectable Hepatocellular Carcinoma Treated with Lenvatinib from a Nationwide Multicenter Study. Cancers (Basel). 2021 May 26;13(11):2608.

[7] Curley SA, Izzo F, Ellis LM, et al.. Radiofrequency ablation of hepatocellular cancer in 110 patients with cirrhosis. Ann Surg. 2000 Sep;232(3):381-91.

[8] Zhang X, Qian H, Qu X,et al.. Efficacy and safety of pembrolizumab/carrelizumab, alone or in combination with chemotherapy in treatment of patients with non-small cell lung cancer: A protocol for evidence-based systematic review and Bayesian network meta-analysis. Medicine (Baltimore). 2021 Jul 23;100(29):e26672.

[9] Mitchell TC, Hamid O, Smith DC, et al.. Epacadostat Plus Pembrolizumab in Patients With Advanced Solid Tumors: Phase I Results From a Multicenter, Open-Label Phase I/II Trial (ECHO-202/KEYNOTE-037). J Clin Oncol. 2018 Nov 10;36(32):3223-3230.

[10] Lohavanichbutr P, Méndez E, Holsinger FC, et al..A 13-Gene Signature Prognostic of HPV-Negative OSCC: Discovery and External Validation. Clin Cancer Res (2013) 19(5):1197–203.

[11] Yu G, Wang L-G, Han Y, et al.. Clusterprofiler: An R Package for Comparing Biological Themes Among Gene Clusters. OMICS (2012) 16 (5):284–7.

[12] Newman AM, Steen CB, Liu CL, et al..Determining Cell Type Abundance and Expression From Bulk Tissues With Digital Cytometry. Nat Biotechnol (2019) 37(7):773–82.

[13] Inoue H, Tani K. Multimodal immunogenic cancer cell death as a consequence of anticancer cytotoxic treatments. Cell Death Differ. 2014 Jan;21(1):39-49.

[14] Zabel M, Willems R, Lubinski A, et al.. Clinical effectiveness of primary prevention implantable cardioverter-defibrillators: results of the EU-CERT-ICD controlled multicentre cohort study. Eur Heart J. 2020 Sep 21;41(36):3437-3447.

[15] Li H, Wang Z, Fang X, Zeng W, et al.. Poroptosis: A form of cell death depending on plasma membrane nanopores formation. iScience. 2022 May 30;25(6):104481.

[16] Huang CY, Chiang SF, Chen WT, et al.. HMGB1 promotes ERK-mediated mitochondrial Drp1 phosphorylation for chemoresistance through RAGE in colorectal cancer. Cell Death Dis. 2018 Sep 26;9(10):1004.